Unclassified

SECURITY CLASSIFICATION OF THIS PAGE (When Data Entered)

AD-A177 150

# REPORT DOCUMENTATION PAGE

READ INSTRUCTIONS BEFORE COMPLETING FORM

| | | |
|---|---|---|
| 1. REPORT NUMBER<br>HIG Contribution 1712 | 2. GOVT ACCESSION NO. | 3. RECIPIENT'S CATALOG NUMBER |
| 4. TITLE (and Subtitle)<br>Hypocenter: An Earthquake Location Method Using Centered, Scaled and Adaptively Damped Least Squares. | | 5. TYPE OF REPORT & PERIOD COVERED<br><br>6. PERFORMING ORG. REPORT NUMBER |
| 7. AUTHOR(s)<br>Barry R. Lienert<br>E. Berg<br>L. Neil Frazer | | 8. CONTRACT OR GRANT NUMBER(s)<br>N00014-82-C-0380 |
| 9. PERFORMING ORGANIZATION NAME AND ADDRESS<br>Hawaii Institute of Geophysics<br>2525 Correa Road<br>Honolulu, Hawaii 96822 | | 10. PROGRAM ELEMENT, PROJECT, TASK AREA & WORK UNIT NUMBERS |
| 11. CONTROLLING OFFICE NAME AND ADDRESS<br>Office of Naval Research<br>Ocean Sciences & Technology<br>Bay St. Louis, MS 39520 | | 12. REPORT DATE<br>July, 1985<br>13. NUMBER OF PAGES<br>12 pages |
| 14. MONITORING AGENCY NAME & ADDRESS(if different from Controlling Office)<br>Office of Naval Research, Branch Office<br>1030 East Green Street<br>Pasadena, CA 91106 | | 15. SECURITY CLASS. (of this report)<br>Unclassified<br>15a. DECLASSIFICATION/DOWNGRADING SCHEDULE |

16. DISTRIBUTION STATEMENT (of this Report)

Approved for public release; distribution unlimited.

17. DISTRIBUTION STATEMENT (of the abstract entered in Block 20, if different from Report)

18. SUPPLEMENTARY NOTES

Published in Bull. Seismol. Soc. Amer., vol. 76, no. 3, p. 771-783, 1986(June).

19. KEY WORDS (Continue on reverse side if necessary and identify by block number)

Earthquake
Hypocenter
Location method
HYPO71 & HYPOINVERSE algorithms
adaptive damping

20. ABSTRACT (Continue on reverse side if necessary and identify by block number)

We present an earthquake location method, HYPOCENTER, which combines features of the two well-known algorithms HYPO71 and HYPOINVERSE, with a new technique which we term adaptive damping. Each column of the linearized condition matrix $T$, which relates changes in arrival time to changes in hypocentral position, is centered and scaled to have zero mean and a norm of one. Origin time is defined as the mean arrival time minus the mean travel time. The three least-squares normal equations for hypocentral coordinates, with diagonal terms equal to one, are then solved iteratively by adding a variable damping factor, $\theta^2$, to their diagonal terms before inversion. If the residual sum of squares increases, we return to the previous iteration, increase $\theta^2$, then try again. This procedure, which we term adaptive damping, always results in residuals which are less than

DD FORM 1 JAN 73 1473 EDITION OF 1 NOV 65 IS OBSOLETE
S/N 0102-014-6601

Unclassified

SECURITY CLASSIFICATION OF THIS PAGE (When Data Entered)

or equal to the HYPO71 or HYPOINVERSE residuals. We demonstrate HYPO-CENTER by comparing it to HYPO71 and HYPOINVERSE using synthetic and real arrival time data for four- and eight-station seismic arrays.

Bulletin of the Seismological Society of America, Vol. 76, No. 3, pp. 771–783, June 1986

# HYPOCENTER: AN EARTHQUAKE LOCATION METHOD USING CENTERED, SCALED, AND ADAPTIVELY DAMPED LEAST SQUARES

By Barry R. Lienert, E. Berg, and L. Neil Frazer


## Abstract

**We present an earthquake location method, HYPOCENTER, which combines features of the two well-known algorithms HYPO71 and HYPOINVERSE, with a new technique which we term 'adaptive damping.' Each column of the linearized condition matrix, which relates changes in arrival time to changes in hypocentral position, is centered and scaled to have zero mean and a norm of one. Origin time is defined as the mean arrival time minus the mean travel time. The three least-squares normal equations for hypocentral coordinates, with diagonal terms equal to one, are then solved iteratively by adding a variable damping factor, $\theta^2$, to their diagonal terms before inversion. If the residual sum of squares increases, we return to the previous iteration, increase $\theta^2$, then try again. This procedure, which we term adaptive damping, always results in residuals which are less than or equal to the HYPO71 or HYPOINVERSE residuals. We demonstrate HYPOCENTER by comparing it to HYPO71 and HYPOINVERSE using synthetic and real arrival time data for four- and eight-station seismic arrays.** (Reprints)


## Introduction

Although the least-squares solution to the earthquake location problem given by Geiger (1910) has been used in various forms for over 70 yr, limitations on modern versions of it such as HYPO71 (Lee and Lahr, 1972) are still apparent. For example, Wesson *et al.* (1971) observed that HYPO71 tended to leave the depths of many hypocenters unchanged from their starting values, while Lomnitz (1977) pointed out that discrepancies in epicenters of the LONGSHOT nuclear explosion determined by different authors exceeded 50 km, even when the same set of arrival time data was used. The advances in geophysical inverse theory (Backus and Gilbert, 1968, 1970) and its formulation in terms of the generalized inverse by Jackson (1972) and Wiggins (1972) led Klein (1978) to write the HYPOINVERSE algorithm. Yet, the algorithm which has still gained the most widespread acceptance is HYPO71, which uses the step-wise statistical regression procedure outlined in Draper and Smith (1981).

In this paper, we examine two of the procedures which differentiate HYPO71 from HYPOINVERSE, namely centering and scaling. We then show how these two procedures can be combined with a damped least-squares solution (Levenburg, 1944; Aki and Lee, 1976) which employs an adaptive damping factor. The combination of centering, scaling, and adaptive damping results in a solution which is in most cases superior to that of either HYPO71 or HYPOINVERSE.

## General Notation

We take as our model a set of seismic stations having known locations and elevations and overlying a one-dimensional stack of constant velocity layers. For any earthquake location, $(x, y, z)$ and origin time, $t_0$, we can calculate the travel time, $T_i(x, y, z)$ to the $i$th station, along with the partial derivatives $\partial T_i/\partial x$, $\partial T_i/\partial y$, $\partial T_i/\partial z$. The differences, $\Delta t_i$, between predicted and observed arrival times,



HIG Contribution No. 1712

$t_i$, will then be

$$\Delta t_i = t_i - T_i(x, y, z) - t_0. \tag{1}$$

We now approximate the residuals, $\Delta t_i$, with the first-order Taylor series expansion of $T_i(x, y, z)$ to obtain a set of weighted residuals, $\tau_i$, i.e.,

$$\tau_i = w_i(t_i - T_i - t_0 - \Delta t_0 - \Delta x \partial T_i/\partial x - \Delta y \partial T_i/\partial y - \Delta z \partial T_i/\partial z) \tag{2}$$

where the $w_i$ are weighting factors normalized so that $\Sigma w_i = 1$. We now adopt the matrix notation

$$\tau = (\tau_1, \tau_2, \cdots, \tau_n)^T$$

$$\Delta t = (w_1 \Delta t_1, \cdots, w_n \Delta t_n)^T$$

and

$$dX_4 = (\Delta t_0, \Delta x, \Delta y, \Delta z).$$

Equation (2) can then be rewritten

$$\tau = \Delta t - T dX_4 \tag{3}$$

where

$$T = \begin{bmatrix} w_1 & w_1 \partial T_1/\partial x & w_1 \partial T_1/\partial y & w_1 \partial T_1/\partial z \\ \vdots & \vdots & \vdots & \vdots \\ w_n & w_n \partial T_n/\partial x & w_n \partial T_n/\partial y & w_n \partial T_n/\partial z \end{bmatrix}.$$

The standard least-squares inverse of equation (3) which minimizes $\sum_i \tau_i^2$ is then

$$dX_4 = (T^T T)^{-1} T^T \Delta t \tag{4}$$

or, in terms of the generalized inverse (Lanczos, 1961)

$$dX_4 = V \Lambda^{-1} U^T \Delta t \tag{5}$$

where the columns of $V$ and $U$ are the eigenvectors of $T^T T$ and $TT^T$, respectively, and $\Lambda$ is the diagonal matrix of common eigenvalues (Jackson, 1972; Wiggins, 1972). Provided we have a first-guess hypocenter, we can apply equation (4) or (5) iteratively to obtain a solution to the location problem. Equations (4) and (5) are the basis of all linearized least-squares solutions to the earthquake location problem.

## Centering

We wish to draw attention to a procedure that is not normally used in geophysical inverse theory, but which leads to a simplification of the inverse problem as well as to improved numerical accuracy. Consider the fourth normal equation obtained by differentiating the sum of squares, $\sum \tau_i^2$, with respect to $t_0$, where the $\tau_i$ are given by equation (2). This will be

$$t_0 + \Delta t_0 = \sum_i w_i t_i - \sum_i w_i T_i - \Delta x \sum_i w_i \partial T_i/\partial x - \Delta y \sum_i w_i \partial T_i/\partial y - \Delta z \sum_i w_i \partial T_i/\partial z \quad (6)$$

which can be rewritten

$$t_0 + \Delta t_0 = \langle t_i \rangle - \langle T_i \rangle - \Delta x \langle \partial T_i/\partial x \rangle - \Delta y \langle \partial T_i/\partial y \rangle - \Delta z \langle \partial T_i/\partial z \rangle \quad (7)$$

where the brackets, $\langle\ \rangle$, represent weighted means. Substituting equation (7) into equation (2), we obtain

$$\tau_i = w_i[t_i - \langle t_i \rangle - (\partial T_i/\partial x - \langle \partial T_i/\partial x \rangle)\Delta x - (\partial T_i/\partial y - \langle \partial T_i/\partial y \rangle)\Delta y - (\partial T_i/\partial z - \langle \partial T_i/\partial z \rangle)\Delta z]. \quad (8)$$

We have replaced the corrected origin time, $t_0 + \Delta t_0$, with the weighted means of each of the remaining terms on the right-hand side of equation (2). This process, termed centering, is a standard procedure used in statistical regression (Draper and Smith, 1981, p. 260). Centering was used by Lee and Lahr (1972) in HYPO71 but not by Klein (1978) in HYPOINVERSE.

We now define the centered condition matrix, $T_c$, as

$$T_c = \begin{bmatrix} w_1(\partial T_1/\partial x - \langle \partial T_i/\partial x \rangle) & w_1(\partial T_1/\partial y - \langle \partial T_i/\partial y \rangle) & w_1(\partial T_1/\partial z - \langle \partial T_i/\partial z \rangle) \\ \vdots & \vdots & \vdots \\ w_n(\partial T_n/\partial x - \langle \partial T_n/\partial x \rangle) & w_n(\partial T_n/\partial y - \langle \partial T_n/\partial y \rangle) & w_n(\partial T_n/\partial z - \langle \partial T_n/\partial z \rangle) \end{bmatrix} \quad (9)$$

which has the least-squares solution

$$dX_3 = (T_c^T T_c)^{-1} T_c^T \Delta t \quad (10)$$

where $dX_3 = (\Delta x, \Delta y, \Delta z)$. It is clear from equation (8) that the mean of the centered residuals, $\tau_i$, is now zero, i.e.,

$$\sum \tau_i = 0. \quad (11)$$

For our final solution, $\Delta x$, $\Delta y$, $\Delta z$, and $\Delta t_0$ are zero. Equation (7) then gives us the equation for origin time

$$t_0 = \langle t_i \rangle - \langle T_i \rangle. \quad (12)$$

## Scaling

Smith (1976) has observed that the condition number (ratio of maximum to minimum eigenvalues) of the matrix $T$ or $(T_c)$ can be improved by scaling the columns of $T$ to all have unit norm. Scaling, like centering, is a standard procedure used in statistical regression (Draper and Smith, 1981, p. 263). We therefore define

$T_{cs}$ by the equation

$$T_{cs} = T_c S^{-\frac{1}{2}} \tag{13}$$

where

$$S = \mathrm{diag}\left(\sum_i T_{ci1}^2, \sum_i T_{ci2}^2, \sum_i T_{ci3}^2\right).$$

We first obtain a solution of $dX_3$ to equation (10) using $T_{cs}$ instead of $T_c$. We then remove the scaling factors from the solution by dividing $dX_3$ by $S$ to obtain the hypocentral corrections $\Delta x$, $\Delta y$, and $\Delta z$. Although scaling is mathematically equivalent to solving equation (10) directly, it always improves the numerical accuracy of the solution. Scaling also removes the dimensionality of parameters such as distance and time which, as Klein (1978) observed, tends to make the eigenvalue for origin time the largest when the $T$ matrix is left uncentered. Furthermore, since the diagonal elements of the $3 \times 3$ symmetric matrix $T_{cs}^T T_{cs}$ are all one, its determinant and inverse have particularly simple forms, suitable for evaluation on a small calculator.

Scaling was used by HYPO71 as part of the step-wise statistical regression procedure, but not by HYPOINVERSE. Jackson (1972) and Wiggins (1972) solved the problem of parameter dimensionality by dividing parameters by suitably chosen variances. However, foreknowledge of parameter variances adds a certain degree of subjectivity to the resulting solution which scaling avoids.

## Damped Least Squares

A least-squares solution to equation (9) can always be found providing that the matrix $T_{cs}^T T_{cs}$ is nonsingular. As $T_{cs}^T T_{cs}$ becomes near-singular, the errors in the corrections $\Delta x$, $\Delta y$, and $\Delta z$, and often the corrections themselves become very large, leading to instability in any iterative scheme. Geophysical inverse theory, as discussed by Backus and Gilbert (1970), directs attention toward the tradeoff between parameter independence (resolution) and parameter variance that always results from stabilization schemes. We have used the scheme termed "damped least squares" by Levenburg (1944), "ridge regression" by Hoerl and Kennard (1970), and "tapered cutoff" by Wiggins (1972). A constant positive term, $\theta^2$, is added to each of the diagonal elements of the matrix $T_{cs}^T T_{cs}$ before inverting it, i.e.,

$$dX = (T_{cs}^T T_{cs} + \theta^2 I)^{-1} T_{cs}^T \Delta t, \tag{14}$$

or in terms of the generalized inverse

$$dX_3 = V(\Lambda^2 + \theta^2 I)^{-1} U^T \Delta t. \tag{15}$$

This scheme was used by Crosson (1976) for the joint solution of hypocentral locations and one-dimensional velocity structure and also by Aki and Lee (1976) for joint solution of two- and three-dimensional velocity structures. The size of the damping term, $\theta^2$, has been the subject of many studies (e.g., Marquardt, 1970; Franklin, 1970; Wichern and Churchill, 1971). In this paper, we adopt an empirical approach to determining the size of $\theta^2$, which we term "adaptive damping." In the earthquake location problem, the primary objective is to minimize the quantity rms $= \sqrt{\Sigma \tau_i^2/N}$. For example, Rowlett and Forsyth (1984), in the algorithm GRIDSEARCH, determine earthquake locations by calculating rms at a large number of points and finding the minimum. We have chosen to use the criterion of minimum rms to determine the size of $\theta^2$. If rms increases in any iteration, we return to the previous solution, increase $\theta^2$, and try again. We term this procedure "adaptive damping." Note that if the generalized inverse given by equation (15) is used, the eigenvalues and eigenvectors do not need to be recalculated when increasing $\theta^2$.

## The HYPOCENTER Algorithm

In addition to adaptive damping, the HYPOCENTER algorithm also incorporates four novel features which are listed below.

1. We start with a $\theta^2$ value of 0.005, which was found empirically to have little effect relative to the least-squares solution. When $\Sigma \tau_i^2$ increases, $\theta^2$ is increased by a factor of four. When $\Sigma \tau_i^2$ is decreasing, we decrease $\theta^2$ by a factor of 0.6, thereby increasing the speed of convergence. The factors used to increase and decrease $\theta^2$ were determined empirically and were not critical to the performance of the algorithm.
2. The following convergence criteria were used: (a) coordinate corrections become <0.05 km and (b) $\Sigma \tau_i^2$ does not decrease after $\theta^2$ has been increased five times in succession.
3. Convergence is first achieved with the depth held fixed. Buland (1976) has pointed out that fixing depth significantly extends the domain of convergence for the location problem. Depth is then freed, and convergence is searched for a second time.
4. Negative depths are treated similarly to increases in $\Sigma \tau_i^2$, i.e., the damping factor is increased. We found that including station elevations in the calculation considerably improved the ability of arrays to locate shallow focus events. This is because the derivatives of arrival times with respect to depth at stations which are coplanar with an event are often all zero, resulting in a singularity in the condition equation matrix.

A summary of the important properties of the algorithms HYPO71, HYPOINVERSE, and HYPOCENTER appears in Table 1. A flowchart of the HYPOCENTER algorithm is given in Figure 1.

## Numerical Examples

To demonstrate the effectiveness of centering and scaling combined with adaptive damping, we have used the following three networks.

NET 1 is a four-station star configuration with one center station and the three others on a 10 km radius, equidistant from each other (Figure 2). The NET 1 configuration was studied by Uhrhammer (1980), who gives its uncertainty and ignorance mappings.

NET 2 consists of eight ocean bottom seismometers (OBS) deployed during 1979 in the Galapagos rift zone by the Hawaii Institute of Geophysics (HIG). The deployment of this array and analysis of the data from it have been described by Milholland (1984).

NET 3 comprises a subset of the landstations which in 1979 were also deployed by HIG near to and in the Petatlan earthquake source region. Some resolution and error maps for NET 3 can be found in Novelo-Casanova *et al.* (1984).

In the first example, we examine improvement in the condition number (i.e., the ratio of the largest to smallest eigenvalue) of the partial derivative matrix $T$, for a hypocenter at 150 km from the center of NET 1 along the line $P1P2$ (Figure 2) and at a depth of 10 km. A $v_P = 5.6$ and $v_S = 3.3$ km/sec half-space velocity model was used. This hypocenter's associated partial derivative matrix $T$, the scaled matrix, $T_s$, and the centered and scaled matrix, $T_{cs}$, have the eigenvalues shown in Table 2. The condition number improves by a factor of 4, when $T$ is centered and by a factor of about 16 when $T$ is both centered and scaled.

The second example examines the effect of damping. Again, NET 1 is used with hypocenters $P1$ to $P9$ (Figure 2) at 50 km intervals along the line $P1P2$ and all at

TABLE 1

COMPARISON OF THE IMPORTANT FEATURES OF THE ALGORITHMS HYPO71, HYPOINVERSE, AND HYPOCENTER

| | HYPO71 | HYPOINVERSE | HYPOCENTER |
|---|---|---|---|
| Centering and scaling | Yes | No | Yes |
| Damping | Step length; $F$-ratio must be >2 for corresponding parameter to be varied | Step length; eigenvectors with eigenvalues <0.016 not used | Damped least-squares with adaptive damping |
| Matrix inversion | Abbreviated Doolittle | Q-R algorithm | Jacobi method |
| Depth variation | Depth fixed if $\lvert \Delta x^2 + \Delta y^2 \rvert > 10$ km | Depth freed when $\lvert \Delta x^2 + \Delta y^2 \rvert < 7$ km | Depth freed when convergence achieved |
| Negative depths ($z + \Delta z < 0$) | Set to 0.5 $\lvert z + \Delta z \rvert$ | Set to $0.5z$ | Return to previous solution and increase damping factor |
| Residual weighting | Jeffrys weighting if rms > 0.1 sec | Cosine taper for 5 rms > $\Delta t$ > 3 rms | Optional bi-square weighting (not used in this study) |
| Distance weighting | No | Yes | No |
| rms increases | No action | Hypocenter moved back toward previous value | Return to previous hypocenter and increase damping |

a depth of 10 km. A two-layer velocity model was used, with a 30-km-thick, $v_P = 6.0$ km/sec upper layer, an 8.0 km/sec lower layer, and a $v_P$ to $v_S$ ratio of 1.78 for both layers. Calculated $P$ and $S$ wave arrival times for each hypocenter were perturbed 10 times with random, Gaussian errors having standard deviations of 0.05 and 0.1 sec, respectively. Each of the resulting 10 sets of arrival times was used to calculate residuals, $\Delta t$, relative to corresponding arrival times for a first-guess hypocenter. This first-guess hypocenter was placed 0.1 km in both horizontal coordinates from the first arrival station and at a depth of 15 km. Equation (14) was then used to iteratively correct the hypocentral parameters using each set of residuals.

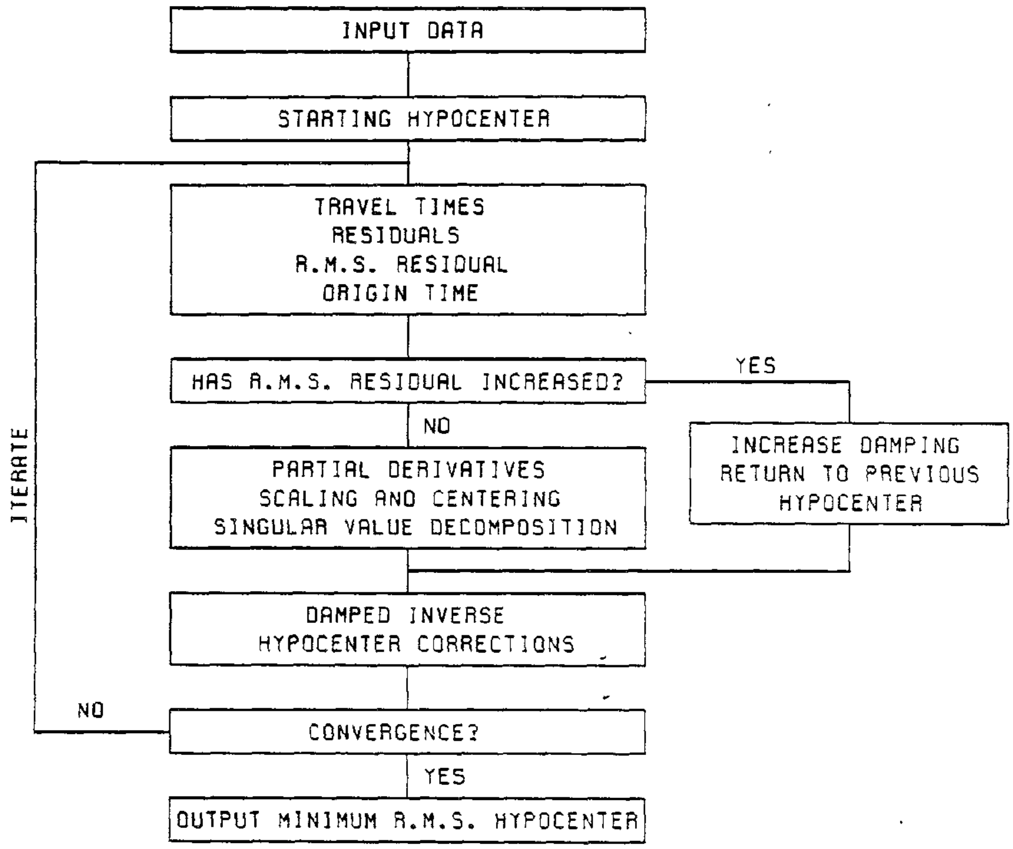


FIG. 1. Flowchart of the HYPOCENTER algorithm.

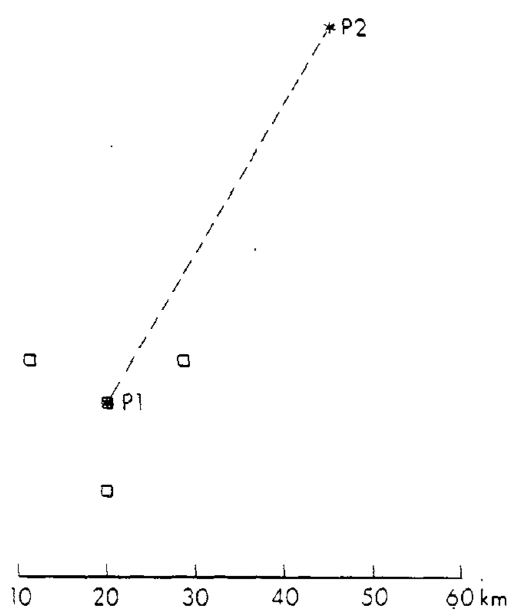


FIG. 2. Location of synthetic epicenters (asterisks) used to test the location algorithms for the NET 1 array. Seismic stations are represented by squares. Hypocenters are all at a depth of 10 km. Epicenters $P3$–$P9$ continue at 50 km intervals along the line $P1P2$.

Shown in Figure 3 are the rms values for the five iterations of equation (14) with $\theta^2 = 0$, corresponding to the least-squares solution. Note that rms decreases on the second iteration for all locations except $P8$ and $P9$. Subsequently, rms increases, particularly on the third iteration. The increases in rms are due to nonlinearity of the travel-time functions $T_i$, i.e., the residuals predicted by the first-order Taylor series expansion of $T_i$ are different from those obtained using equation (1). Step length damping, where some fixed fraction of $dX_3$ or $dX_4$ is used as a correction, has been suggested by Buland (1976) as a solution to this problem and was used in

TABLE 2
CALCULATED EIGENVALUES OF $T^TT$ FOR THE SYNTHETIC EVENT $P4$ (SEE FIGURE 2)

| Partial Derivative Matrix | $\lambda_1$ | $\lambda_2$ | $\lambda_3$ | $\lambda_4$ | $\lambda_{max}/\lambda_{min}$ |
|---|---|---|---|---|---|
| No centering or scaling | 2.89 | 0.241 | 0.168 | 0.019 | 151 |
| Scaled, not centered | 1.85 | 0.724 | 0.228 | 0.045 | 41 |
| Scaled and centered | — | 1.438 | 0.954 | 0.148 | 10 |

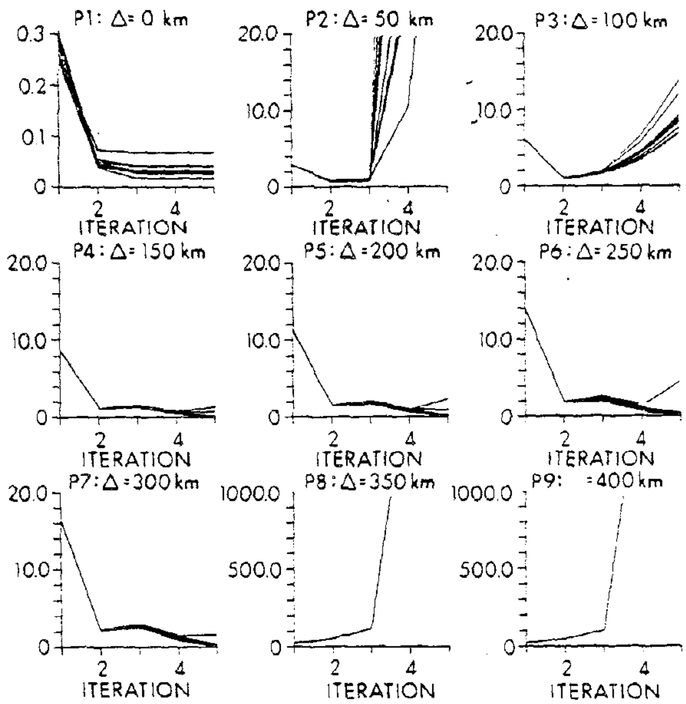


FIG. 3. Plots of changes in the rms residual for the synthetic events shown in Figure 1, and $\theta^2 = 0$ in equation (14). Note the changes of scale on the rms axis for different locations.

the algorithms HYPO71 and HYPOINVERSE (Table 1). However, step length damping breaks down if $\Delta x$, $\Delta y$, or $\Delta z$ have the wrong sign. Damped least squares has the advantage of providing step direction as well as step-length damping (Marquardt 1970).

Figure 4 demonstrates the effect of a damping factor of $\theta^2 = 1$ in equation (14), using the same data set as in Figure 3. The initial decrease in rms is smaller compared to the undamped results in Figure 3, but divergence is prevented at all but the most distant locations $P8$ and $P9$, 350 and 400 km from the center of the

20 km diameter array. Even choosing $\theta^2$ values as large as 50, or fixing depth as suggested by Buland (1976), were unsuccessful at preventing divergence at the $P8$ and $P9$ locations. We obtained convergence only by using starting locations closer to the theoretical hypocenters. Such improved first-guess locations could be obtained using the order of arrival times (Anderson 1981), or a wave front approach direction and $S$-$P$ arrival time differences.

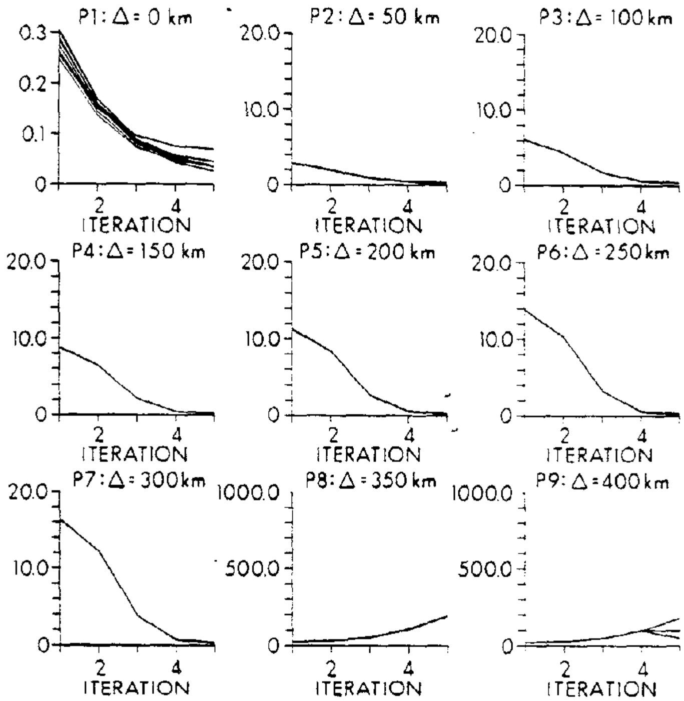


FIG. 4. Changes in rms for damped least-squares solutions ($\theta^2$ = 1) of the same data set used in Figure 2.

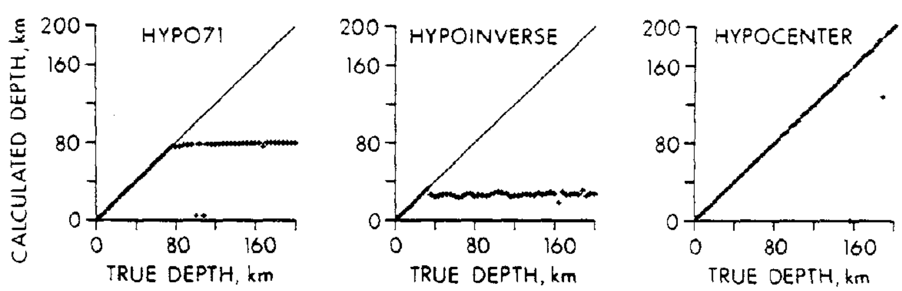


FIG. 5. Calculated depth versus true depth as determined by HYPO71, HYPOINVERSE, and HYPOCENTER for synthetic hypocenters directly beneath the center station of the NET 1 array shown in Figure 1. A half-space velocity model with $v_P$ = 5.6 km/sec and $v_S$ = 3.3 km/sec was used to generate the synthetic hypocenters.

The third example is a test on synthetic data for NET 1, a half-space velocity structure ($v_P = 5.6$, $v_S = 3.3$ km/sec), Gaussian arrival time errors of 0.05 sec in $P$ and 0.1 sec in $S$, and hypocenters located at 4 km increments in depth below the central station ($P1$ in Figure 2). Calculated versus true depths are compared in Figure 5 for HYPO71, HYPOINVERSE, and HYPOCENTER, using a first-guess depth of 5 km. HYPOINVERSE fails to converge when the true depth is greater

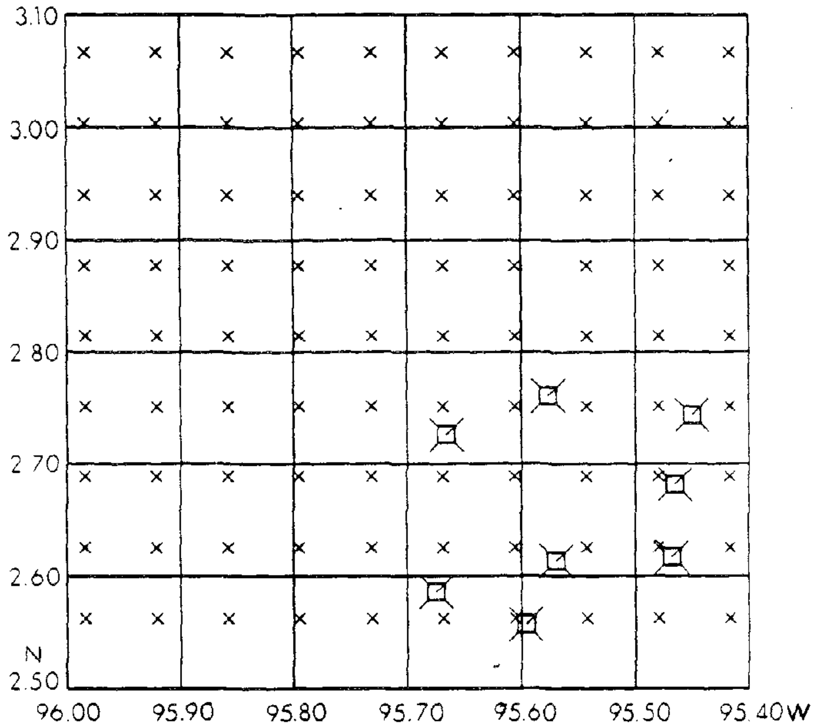


FIG. 6. Locations of synthetic earthquakes (crosses) relative to the NET 2 array (crossed squares) which we used for the comparison of algorithms HYPO71, HYPOINVERSE, and HYPOCENTER. Hypocenters are all at zero depth.

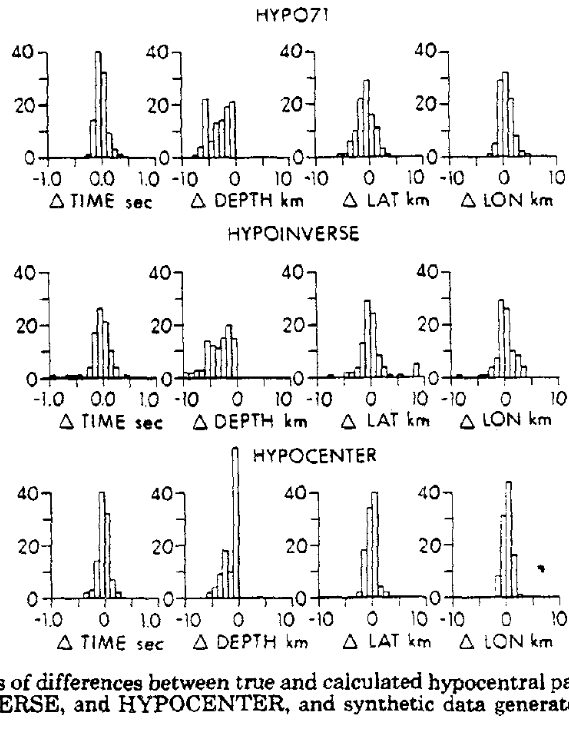


FIG. 7. Histograms of differences between true and calculated hypocentral parameters obtained using HYPO71, HYPOINVERSE, and HYPOCENTER, and synthetic data generated for the events shown in Figure 6.

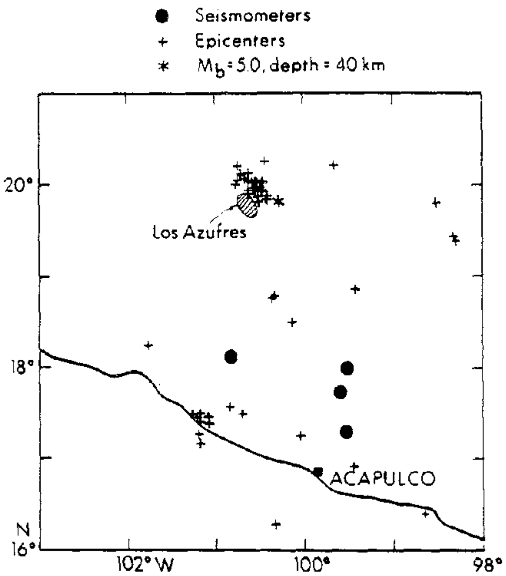


FIG. 8. Map showing the Petatlan subarray [NET 3 (solid circles)] and epicenters (crosses) as determined by HYPO71. Also shown is the Los Azufres geothermal area, a nearby $M = 5.2$ event (indicated by the asterisk) and its associated aftershocks.

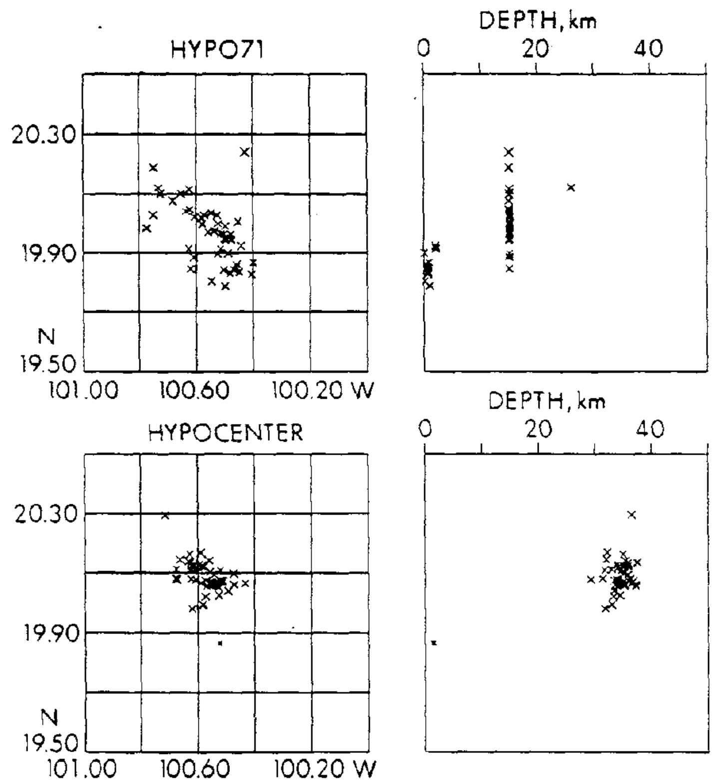


FIG. 9. Expanded epicenter maps and north-south cross-section plots of the Los Azufres aftershock sequence as determined by HYPO71 and HYPOCENTER.

than about 40 km, while HYPO71 fails at depths of greater than 50 km. Changing the value for the $F$-ratio test from 2 to 0.5 considerably improved HYPO71's performance in this example, suggesting that the default setting of 2 may be somewhat high, at least for Gaussian errors. Clearly HYPO71 and HYPOINVERSE performance is unsatisfactory, as the $S$-$P$ arrival time difference always provides good depth control in this particular example.

The fourth example uses synthetic $P$ and $S$ wave arrival times for the Galapagos OBS array NET 2, again with 0.05 and 0.1 sec Gaussian errors in $P$ and $S$, respectively. Hypocenters were placed at the grid points shown in Figure 6 and at zero depth. Figure 7 compares differences between true and calculated locations and origin times for HYPO71, HYPOINVERSE, and HYPOCENTER. Note the better performance of HYPOCENTER, indicated by smaller differences in true versus calculated coordinates, especially depth.

We now turn our attention to real data collected by the NET 3 Petatlan subarray. Figure 8 shows the subarray and the HYPO71 epicenters obtained using a five-layer velocity model. We concentrate attention on the northern part of that map, i.e., on a cluster of aftershocks which followed an $M_b = 5$ earthquake occurring close to the Los Azufres geothermal area. Figure 9 compares in detail epicenters and depths determined by the two algorithms. HYPO71 mostly failed to vary depth at all from its initial value of 15 km, where HYPOCENTER locations show tight clustering at a depth of 35 km in a much smaller volume than HYPO71. Further examples of the improved performance of the HYPOCENTER algorithm have been described by Milholland (1984) and Ambos (1984).

An IBM-PC diskette copy of the Fortran program HYPOCENTER can be obtained from the first author upon request. The program processes input data which is identical in format to that read by HYPO71.

## Conclusions

We have demonstrated that both improved convergence and improved numerical stability can be achieved for the earthquake location problem by centering and scaling of the observation matrix in combination with adaptive damping of the least-squares solution.

Centering, scaling, and adaptive damping combine to provide an effective and simple solution to the problem of locating earthquakes.

## Acknowledgments

We acknowledge many helpful discussions with HIG staff and students, particularly Robert Cessaro and Phillip Milholland. We acknowledge and appreciate the helpful and extensive comments of two anonymous reviewers as well as those of Fred Klein and Rita Pujalet. This research was supported by the Office of Naval Research and by the National Science Foundation under Grant EAR-82-13745.

## References

Aki, K. and W. H. K. Lee (1976). Determination of three-dimensional velocity anomalies under a seismic array using first $P$ arrivals times from local earthquakes. I. A homogeneous initial model, *J. Geophys. Res.* **81**, 4381–4399.

Ambos, E. L. (1984). Application of ocean bottom seismometer data to the study of forearc and transform fault systems, *Ph.D. Dissertation*, University of Hawaii, Honolulu, Hawaii.

Anderson, K. R. (1981). Epicentral location using arrival time order, *Bull. Seism. Soc. Am.* **71**, 541–546.

Backus, G. and F. Gilbert (1968). The resolving power of gross earth data, *Geophys. J. R. Astr. Soc.* **16**, 169–205.

Backus, G. and F. Gilbert (1970). Uniqueness in the inversion of inaccurate gross earth data, *Phil. Trans. R. Soc. Lond.* **266A**, 123–192.

Buland, R. (1976). The mechanics of locating earthquakes, *Bull. Seism. Soc. Am.* **66**, 173–187.

Crosson, R. S. (1976). Simultaneous least squares estimation of hypocenter and velocity parameters, *J. Geophys. Res.* **81**, 3036–3046.

Draper, N. R. and H. Smith (1981). *Applied Regression Analysis*, second edition, John Wiley and Sons, Inc., New York.

Franklin, J. N. (1970). Well-posed stochastic extensions of ill-posed linear problems, *J. Math. Anal. Appl.* **31**, 682–716.

Geiger, L. (1910). Herbsetimmung bei Erdbeben aus den Ankunfzeiten, *K. Gessel. Wiss. Goett.* **4**, 331–349.

Hoerl, A. E. and R. W. Kennard (1970). Ridge regression: biased estimation for nonorthogonal problems, *Technometrics* **12**, 55–67.

Jackson, D. D. (1972). Interpretation of inaccurate, insufficient and inconsistent data, *Geophys. J. R. Astr. Soc.* **28**, 97–109.

Klein, R. W. (1978). Hypocenter Location Program HYPOINVERSE Part I: Users Guide to Versions 1, 2, 3 and 4, *U.S. Geol. Surv. Open-File Rept. 78-694.*

Lanczos, C. (1961). *Linear Differential Operators*, D. Van Nostrand, London, 546 pp.

Lee, W. H. K. and J. C. Lahr (1972). HYPO71: a computer program for determining hypocenter, magnitude, and first motion pattern of local earthquakes, *U.S. Geol. Surv. Open-File Rept. 75-311.*

Levenburg, K. (1944). A method for the solution of certain non-linear problems in least-squares, *Quart. Appl. Math.* **2**, 164–168.

Lomnitz, C. (1977). A fast epicenter location program, *Bull. Seism. Soc. Am.* **67**, 425–431.

Marquardt, D. W. (1970). Generalized inverses, ridge regression, biased linear estimation, and nonlinear estimation, *Technometrics* **12**, 591–611.

Milholland, P. D. (1984). Seismicity of the 95.5°W Galapagos propagating rift, *Ph.D. Dissertation*, University of Hawaii, Honolulu, Hawaii.

Novelo-Casanova, D. A., V. Hsu, E. Berg, C. E. Helsley, and J. F. Gettrust (1984). Aftershock activity of the Petatlan earthquake: the first 54 hours, *Bull. Seism. Soc. Am.* **74**, 2451–2461.

Rowlett, H. and D. W. Forsyth (1984). Recent faulting and microearthquakes at the intersection of the Vema fracture and mid-Atlantic ridge, *J. Geophys. Res.* **89**, 6079–6094.

Smith, E. G. C. (1976). Scaling the equations of condition to improve conditioning, *Bull. Seism. Soc. Am.* **66**, 2075–2081.

Uhrhammer, R. A. (1980). Analysis of small seismographic station networks, *Bull. Seism. Soc. Am.* **70**, 1369–1379.

Wesson, R. L., W. H. K. Lee, and J. F. Gibbs (1971). Aftershocks of the San Fernando, California earthquake of February 9, 1971, *U.S. Geol. Surv. Profess. Paper 733*, U.S. Government Printing Office, Washington, D.C., 24–29.

Wichern, D. W. and G. A. Churchill (1978). A comparison of ridge estimators, *Technometrics* **20**, 301–311.

Wiggins, R. A. (1972). The general linear inverse problem: implications of surface waves and free oscillations for earth structure, *Rev. Geophys. Space Phys.* **10**, 251–285.

UNIVERSITY OF HAWAII AT MANOA
HAWAII INSTITUTE OF GEOPHYSICS
2525 CORREA ROAD
HONOLULU, HAWAII 96822
CONTRIBUTION NO. 1712

Manuscript received 16 September 1985